

# Close-coupled calculation of collisions of magnetostatically trapped metastable helium atoms

V. Venturi and I. B. Whittingham

*School of Computer Science, Mathematics and Physics, James Cook University, Townsville 4811, Australia*

P. J. Leo

*Atomic Physics Division, National Institute of Standards and Technology, Gaithersburg, Maryland 20899*

G. Peach

*Department of Physics and Astronomy, University College London, London WC1E 6BT, United Kingdom*

(Received 2 July 1999)

A quantum-mechanical close-coupled calculation for collisions of spin-polarized triplet helium atoms in a magnetostatic trap is presented in which the Penning and associative ionization processes are represented by a complex optical potential. The rate coefficients for the spin relaxation and relaxation-induced Penning ionization processes for a range of magnetic fields and temperatures, spanning the cold and ultracold temperature regimes, have been calculated and the sensitivity of these results to uncertainties in the molecular potentials and autoionization width investigated. The rate constants for both elastic and inelastic processes were found to be particularly sensitive to the short-range  $^5\Sigma_g^+$  molecular potential and, to a lesser extent, the rate constants for relaxation-induced Penning ionization displayed sensitivity to the short-range form of the  $^1\Sigma_g^+$  molecular potential and the autoionization width. [S1050-2947(99)07012-2]

PACS number(s): 34.50.-s, 32.80.Dz, 32.10.Hq

## I. INTRODUCTION

The attainment of Bose-Einstein condensation [1] and the cooling and trapping of neutral atoms [2] has produced a growing theoretical and experimental interest in atomic collisions in the cold and ultracold temperature domains, particularly in the presence of external fields. Studies of these atomic collisions are motivated not only by the consequences for the performance of cooling and trapping applications but also by the desire to gain a better understanding of the fundamental nature of cold and ultracold collisions.

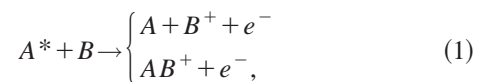
Inelastic collisions can be an important source of loss processes and limit the achievable density of trapped atoms. Knowledge of collision dynamics and the ability to manipulate collisions using external fields can be used to minimize trap loss. There are several unique features of cold and ultracold collisions that are of interest and require particular consideration: the onset of quantum threshold behavior, the sensitivity of the relative motion of the colliding atoms to the molecular potentials, and the modification of collision dynamics due to forces induced by external fields or the occurrence of spontaneous emission of excited states [3].

Although a majority of the theoretical and experimental investigations of cold and ultracold collisions have focused on alkali-metal systems [4], there is considerable interest in metastable rare gases. Metastable helium has been the subject of several trapping and cooling experiments [5–11], and spin-polarized triplet helium  $\text{He}^*(2^3S)\uparrow$  is a possible candidate for Bose-Einstein condensation [6,12,13]. There has also been a focus on producing an intense, slow, and well-collimated beam of metastable helium atoms [14,15] which can be used in molecular spectroscopy, atom optics experiments, and to investigate scattering processes that are inaccessible using conventional techniques. Experimental studies of optical collisions of cold metastable helium atoms [16–18] are also of great importance as they yield information on

the long-range interactions in these systems, and further studies have been proposed [19]. Laser cooling and trapping of neon [20] and krypton [21] metastable atoms have been carried out and cold collisions in metastable xenon [22] and krypton [23] have been studied experimentally. Ionizing collisions in optical lattices for metastable krypton and argon [24] and metastable xenon [25] have also been experimentally investigated. By contrast, there have only been a few theoretical studies of cold collisions for rare-gas metastables [3,12,13,26,27].

Rare-gas metastable atoms offer several attractive features for cooling and trapping techniques and for both theoretical and experimental studies of cold collisions [3,28]. A majority of the rare-gas isotopes of interest have less complex structures than the alkali-metal species, due partly to the absence of hyperfine structure. This greatly simplifies theoretical studies by reducing the number of molecular states that need to be considered. The long radiative lifetimes of the lowest metastable rare-gas states enable them to be viewed as effective ground states, and the existence of convenient optical transitions to other states is ideal for laser-cooling techniques [6,20]. The high excitation energies of metastable atoms also provide an experimental advantage by enabling efficient and accurate detection.

The ionization reactions which occur in collisions of rare-gas metastable atoms are also of great interest,



where the first of these processes is Penning ionization (PI) and the second is associative ionization (AI). These ionization processes are an important source of loss of trapped atoms particularly for unpolarized samples [3]. There have only been a few detailed studies of these processes at sub-

thermal energies [29,30] and there is still much to understand about them. The effects of autoionization processes can be included in theoretical collision studies by a complex optical potential [30,31], coupling to an artificial channel [32], or a perfectly absorbing boundary at a particular internuclear separation [12].

Helium is a particularly attractive prospect for studying fundamental aspects of ultracold collisions [6] and because it has only one active electron, molecular potentials can be computed to greater accuracy than is possible for most other systems. Despite the fact that there have been several experiments involving cold metastable helium, very few theoretical collision studies exist. Julienne and Mies [3] have calculated the threshold rate coefficient for Penning ionization for unpolarized metastable triplet helium and Fedichev *et al.* [12,13] have investigated the feasibility of Bose-Einstein condensation in spin-polarized metastable triplet helium gas. There has been recent interest in the optical suppression of collisional effects which has been demonstrated theoretically and experimentally for metastable xenon [22,27] and experimentally for krypton [23]. However, optical shielding has yet to be studied in metastable helium systems.

A detailed study of cold metastable helium collisions requires fully quantum-mechanical methods because the onset of quantum threshold behavior cannot be described semiclassically [3]. For  $^3S_1$  helium metastables in a magnetostatic trap, a time-independent quantum close-coupled formalism is an appropriate choice for such a study. Such a formalism is also applicable to magneto-optically trapped helium metastables provided certain conditions are satisfied. For magneto-optically trapped helium metastables, excited  $^3P$  atoms exist and the collision time at these low temperatures can be longer than the radiative lifetime of the excited state, implying that spontaneous decay of colliding atoms in the excited state and recycling of population between the ground and excited states may have to be considered. There are many different theoretical approaches available for studying cold collisions in the presence of an optical field. A detailed comparison of the various methods with some discussion of the limitations of the different treatments can be found in Refs. [33–35]. In the weak-field limit, recycling can be ignored and in the case of large laser detunings it has been shown [36] that spontaneous emission can be neglected. A quantum-mechanical close-coupled approach is only valid within these limits, when population recycling can be neglected and spontaneous emission is either negligible or sufficiently small [3]. In the latter case the quantum complex potential method can be used to represent the effects of excited-state decay by a complex potential term [34,37–39]. The quantum complex potential method has several advantages over other available approaches. It is a fully quantum-mechanical treatment and avoids the ambiguity associated with the initial velocity of the excited state that arises when the atomic motion is treated classically [37]. The quantum complex potential method is capable of treating bound-state resonance structure which is not practicable with wavepacket methods [39,40] and computationally this approach may be much less demanding than fully quantum density matrix and Monte Carlo wave function methods. This ap-

proach also offers the option of applying multichannel quantum defect theory to gain further insight into quantum threshold behavior [3].

This present investigation considers inelastic processes involving metastable triplet helium atoms in the presence of a magnetic field. This system is ideal for the development of a quantum close-coupled approach to cold collisions in the presence of an external field as the numerical and computational techniques can be validated against existing results [12], obtained using a perturbative treatment of the spin-dipole interaction. The formalism has been structured with the aim of extending this theoretical and numerical approach to calculations for collisions of cold metastable helium atoms in the presence of an optical field. Although there exist additional issues to be considered for collisions in laser fields, it is believed that the approach developed here deals with some of the theoretical and computational issues related to the presence of autoionization processes and an external field.

The primary interest in ultracold collisions in a spin-polarized metastable triplet helium gas has arisen from the suggestion that it is a possible candidate for Bose-Einstein condensation [6,12] because the large, positive scattering length calculated for the elastic interaction of two  $\text{He}^*(2^3S)\uparrow$  atoms implies stability of the condensate. Spin polarization also overcomes the high threshold rate coefficient for Penning ionization for unpolarized metastable triplet helium, which has been estimated to be  $>5 \times 10^{-10} \text{ cm}^3 \text{ sec}^{-1}$  [3], as it reduces the rate of Penning ionization by ensuring that the colliding atoms are initially in the  $^5\Sigma_g^+$  molecular state, from which these autoionization processes are spin forbidden. References [12,13] have predicted the Penning ionization rate to be five orders of magnitude smaller for polarized atoms than for nonpolarized atoms. The inelastic collisions in polarized metastable triplet helium are mediated by the spin-dipole interaction and can lead to the loss of atoms from the trap. Spin relaxation can change the spin projection of the quasimolecule so that it is no longer confined by the magnetic field or can result in a change in the molecular state of the colliding atoms from the  $^5\Sigma_g^+$  to  $^1\Sigma_g^+$  state, from which there is a high probability of Penning ionization. The latter process is known as relaxation-induced Penning ionization. Investigation of these collision processes is important because the achievable density of atoms within the trap is determined by the rates of these inelastic collisions and the efficiency of the evaporative cooling process depends on the elastic collision cross section.

The  $^5\Sigma_g^+$  and  $^1\Sigma_g^+$  adiabatic molecular potentials required in this close-coupled scattering calculation are those obtained by Stärck and Meyer [41] and Müller *et al.* [30], respectively. Since the  $^5\Sigma_g^+$  potential is claimed to be the more accurate of the two, the  $^1\Sigma_g^+$  potential was modified to have the same long-range form as the  $^5\Sigma_g^+$  potential. The short-range form given by Müller *et al.* [30] was maintained for  $R < 12 a_0$ , and for  $R \geq 12 a_0$  the  $^1\Sigma_g^+$  potential differed from the  $^5\Sigma_g^+$  potential by an exchange energy term. The sensitivity of the calculations to the uncertainty in these molecular potentials has been numerically investigated and will be discussed further when the results of the calculations are presented.

This paper is organized as follows. In Sec. II the close-coupled scattering formalism is developed and theoretical issues relating to the occurrence of autoionization processes and the presence of the external magnetic field are considered. Following a discussion of the choice of an appropriate molecular basis, details of the particular molecular basis selected for this investigation are given and explicit expressions provided for the Hamiltonian matrix elements. The scattering boundary conditions and the calculation of cross sections and rate constants for the spin relaxation and relaxation-induced Penning ionization processes from non-unitary scattering matrices are discussed.

The FARM (flexible asymptotic  $\mathcal{R}$ -matrix) package [42] of routines used to perform the numerical calculations is described in Sec. III, together with some details of the performance of individual routines in the ultracold temperature regime. The results of the numerical calculations and details of investigations into the sensitivity of the results to variations of the molecular potentials and autoionization width are presented in Sec. IV. Finally, in Sec. V, a summary of the outcomes of this investigation is given. General expressions for the various Hamiltonian matrix elements are evaluated in the Appendix.

## II. CLOSE-COUPLED SCATTERING FORMALISM

The total Hamiltonian describing the collision between two atoms in the presence of an external magnetic field is

$$H = T + H_{\text{rot}} + H_{\text{el}} + H_{\text{so}} + H_{\text{Zee}} + H_{\text{sd}}, \quad (2)$$

where  $T$  is the radial kinetic-energy operator of the two atoms,  $H_{\text{rot}}$  is the kinetic-energy operator of the rotating molecule, and the electronic Hamiltonian is  $H_{\text{el}} = H_1 + H_2 + H_{12}$ , for which  $H_1$  and  $H_2$  are the Hamiltonians for the unperturbed atoms and  $H_{12}$  is the Hamiltonian for the electrostatic interaction between the two atoms.  $H_{\text{so}}$ ,  $H_{\text{Zee}}$ , and  $H_{\text{sd}}$  are the Hamiltonians for the spin-orbit, Zeeman, and spin-dipole interactions, respectively.

The quantum close-coupling theory involves the expansion of the total wave function in terms of a complete set of molecular basis states and a set of unknown radial functions. The molecular basis functions must be chosen such that in the asymptotic limit  $R \equiv |\mathbf{R}| \rightarrow \infty$ , where  $\mathbf{R}$  is the internuclear separation vector, the motion of the two-atom system is properly described.

### A. Molecular basis

In the absence of an external field, the two-atom system is described asymptotically by the states

$$|jM_j l M_l\rangle = Y_{l, M_l}(\hat{\mathbf{R}}) |jM_j\rangle. \quad (3)$$

The set of spherical harmonics  $Y_{l, M_l}(\hat{\mathbf{R}})$  represents the relative rotational motion of the nuclei. Here  $l$  and  $M_l$  are, respectively, the quantum numbers associated with the relative rotational angular momentum  $\mathbf{l}$  and its projection onto the quantization axis  $Oz$  in the space-fixed frame  $Oxyz$ . The states  $|jM_j\rangle$  describe the electronic state of the two atoms. The quantum numbers  $j$  and  $M_j$  are associated with the total

electronic angular momentum  $\mathbf{j}$  and its projection onto the space-fixed quantization axis, respectively.

For the  $LS$  coupling scheme appropriate to helium, the total electronic angular momentum  $\mathbf{j}$  is the vector sum of the total orbital angular momentum  $\mathbf{L}$  and the total spin angular momentum  $\mathbf{S}$ . The states  $|jM_j\rangle$  are therefore expressible in the form

$$|jM_j\rangle = \sum_{M_L, M_S} C(LSj; M_L M_S M_j) |LM_L SM_S\rangle, \quad (4)$$

where  $C(j_1 j_2 j_3; m_1 m_2 m_3)$  is a Clebsch-Gordan coefficient [43] and  $M_L$  and  $M_S$  are the projections of  $\mathbf{L}$  and  $\mathbf{S}$ , respectively, onto the  $Oz$  axis. In terms of the states of the individual atoms, the states appearing in Eq. (4) are given by

$$\begin{aligned} & |LM_L SM_S\rangle \\ &= \sum_{M_{L_1}, M_{L_2}} \sum_{M_{S_1}, M_{S_2}} C(L_1 L_2 L; M_{L_1} M_{L_2} M_L) \\ & \quad \times C(S_1 S_2 S; M_{S_1} M_{S_2} M_S) |L_1 M_{L_1}\rangle |L_2 M_{L_2}\rangle \\ & \quad \times |S_1 M_{S_1}\rangle |S_2 M_{S_2}\rangle, \end{aligned} \quad (5)$$

where the subscripts 1 and 2 refer to the individual atoms.

The molecular states which satisfy the above requirements in the asymptotic limit are

$$|R, jM_j l M_l\rangle = Y_{l M_l}(\hat{\mathbf{R}}) |R, jM_j\rangle, \quad (6)$$

where

$$|R, jM_j\rangle \underset{R \rightarrow \infty}{\sim} |jM_j\rangle, \quad (7)$$

$$|R, jM_j l M_l\rangle \underset{R \rightarrow \infty}{\sim} |jM_j l M_l\rangle. \quad (8)$$

The label  $R$  is used to distinguish the molecular state from the two-atom state to which it dissociates adiabatically.

In the absence of an external field, the quantum number  $J$  associated with the total angular momentum of the system  $\mathbf{J} = \mathbf{l} + \mathbf{j}$  is a good quantum number and it is convenient to define the total angular momentum states

$$|R, JM_j j l\rangle = \sum_{M_l M_j} C(j l J; M_j M_l M_J) Y_{l, M_l}(\hat{\mathbf{R}}) |R, jM_j\rangle, \quad (9)$$

where  $M_J$  is the projection of  $\mathbf{J}$  onto the  $Oz$  axis. This molecular basis is the Hund's case ( $e$ ) basis which describes the states of infinitely separated noninteracting atoms colliding with relative angular momentum  $l$ .

The states  $|R, jM_j\rangle$  may be expressed in terms of molecular basis states in the body-fixed frame

$$|R, jM_j\rangle = \sum_{\Omega_j} D_{M_j, \Omega_j}^{j*}(\phi, \theta, 0) |R, j\Omega_j\rangle, \quad (10)$$

where

$$|R, j\Omega_j\rangle = \sum_{\Omega_L \Omega_S} C(LSj; \Omega_L \Omega_S \Omega_j) |R, L\Omega_L S\Omega_S\rangle \quad (11)$$

and  $\Omega_L$ ,  $\Omega_S$ , and  $\Omega_j$  denote the projection of  $\mathbf{L}$ ,  $\mathbf{S}$ , and  $\mathbf{j}$  onto the internuclear axis  $OZ$  in the body-fixed frame  $OXYZ$ . Use of Eq. (10) in Eq. (9) enables the states given in Eq. (9) to be expressed in the form

$$|R, JM_{Jj}l\rangle = \left(\frac{2l+1}{4\pi}\right)^{1/2} \sum_{\Omega_j} C(jlJ; \Omega_j 0 \Omega_j) \times D_{M_J, \Omega_j}^{J*}(\phi, \theta, 0) |R, j\Omega_j\rangle. \quad (12)$$

The total angular momentum basis is ideal for dealing with collisions in the absence of an external field as the total Hamiltonian is then diagonal in  $J$  and independent of  $M_J$ , thus yielding a set of close-coupled equations which only have to be solved for each value of  $J$ . In the presence of an external magnetic or optical field, the total angular momentum  $\mathbf{J}$  is no longer conserved and states with  $J$  and  $J' = J, J \pm 1$  are coupled together. The total angular momentum states  $|R, JM_{Jj}l\rangle$  therefore do not form an adequate molecular basis in that the total Hamiltonian is not asymptotically diagonal in this basis and an infinite set of coupled equations results. Whereas for the magnetostatic trapping case the Zeeman interaction and hence the total Hamiltonian can be made asymptotically diagonal by using the uncoupled basis  $|jM_jlM_j\rangle$  rather than the total angular momentum basis, for the magneto-optical trapping case there is no basis in which the total Hamiltonian is exactly asymptotically diagonal. In many studies it is assumed that the external laser field is weak, thus allowing the manifold of coupled states to be reduced to just those involving  $J$  and  $J \pm 1$ . However, in general, the determination of the number of coupled states and the asymptotically diagonal basis for the magneto-optical case must be done numerically. For this reason this procedure has been implemented for the present studies of magnetostatic trapping as the formalism and computational techniques developed can be tested against results obtained using the uncoupled  $|jM_jlM_j\rangle$  basis and against existing calculations using a perturbative treatment of the spin-dipole interaction. In order to obtain the appropriate basis states, constructed from the total angular momentum states defined above, the matrix elements of the various components of the total Hamiltonian (2) need to be considered first.

### B. Matrix elements of the Hamiltonian components

Explicit evaluations of matrix elements of the various terms in the total Hamiltonian are obtained using the expressions for the channel states given in either Eq. (9) or Eq. (12). The expressions for the matrix elements that follow are for the specific case of collisions between metastable triplet helium atoms. More general expressions are provided in the Appendix.

The radial kinetic-energy operator appearing in Eq. (2) has the form  $T = -\hbar^2/(2\mu R) \times d^2/dR^2 R$  and the rotational Hamiltonian is given by  $H_{\text{rot}} = \mathbf{I}^2/(2\mu R^2)$ , where  $\mu$  is the reduced mass of the collision system. Within the Born-Oppenheimer approximation and the pure precession approximation, which assumes  $l$  to be a good quantum number

for all internuclear separations  $R$ , the matrix elements of these two Hamiltonian terms are

$$\begin{aligned} & \langle R, J' M_{J'} j' l' | (T + H_{\text{rot}}) | R, J M_{Jj} l \rangle \\ &= \left[ \frac{-\hbar^2}{2\mu R} \frac{d^2}{dR^2} R + \frac{\hbar^2 l(l+1)}{2\mu R^2} \right] \delta_{J, J'} \delta_{M_{J'}, M_{Jj}} \delta_{j, j'} \delta_{l, l'}. \end{aligned} \quad (13)$$

The matrix elements of the electronic Hamiltonian can be expressed in terms of the adiabatic molecular potentials  $^{2S+1}V_{\Lambda}(R)$  for the quasimolecular states formed during the collision of two atoms, defined by

$$\begin{aligned} & (H_1 + H_2 + H_{12}) | R, L\Omega_L S\Omega_S \rangle \\ &= [E^{\infty} + ^{2S+1}V_{\Lambda}(R)] | R, L\Omega_L S\Omega_S \rangle, \end{aligned} \quad (14)$$

where  $E^{\infty}$  is the total internal energy of the asymptotically free atoms and  $\Lambda = \Sigma, \Pi, \Delta, \dots$  for  $|\Omega_L| = 0, 1, 2, \dots$ . Using Eq. (14) and the fact that all the  $\text{He}^*(2^3S)$ - $\text{He}^*(2^3S)$  quasimolecular states are  $\Sigma$  states, the electronic Hamiltonian matrix elements are given by

$$\begin{aligned} & \langle R, J' M_{J'} j' l' J' | H_{\text{el}} | R, J M_{Jj} l J \rangle \\ &= [E^{\infty} + ^{2S+1}V_{\Sigma}(R)] \delta_{J, J'} \delta_{M_{J'}, M_{Jj}} \delta_{j, j'} \delta_{l, l'}, \end{aligned} \quad (15)$$

where now  $j = S$ .

Also, since all quasimolecular states are  $\Sigma$  states in this investigation, the matrix elements for the spin-orbit interaction

$$H_{\text{so}} = a(R) \mathbf{L} \cdot \mathbf{S} = \frac{1}{2} a(R) [\mathbf{j}^2 - \mathbf{L}^2 - \mathbf{S}^2] \quad (16)$$

will be zero.

The spin-dipole interaction arises from the interaction of the spin magnetic dipole moments of two electrons and is given by [44]

$$H_{\text{sd}} = \frac{\mu_0 (g_s \mu_B)^2}{4\pi \hbar^2} \frac{1}{R^5} [(\mathbf{S}^{(1)} \cdot \mathbf{S}^{(2)}) R^2 - 3(\mathbf{S}^{(1)} \cdot \mathbf{R})(\mathbf{S}^{(2)} \cdot \mathbf{R})], \quad (17)$$

where  $\mathbf{S}^{(i)}$  ( $i = 1, 2$ ) are the spin operators for the two electrons and  $g_s$  is the electron spin gyromagnetic ratio. Only the spin-dipole interaction is nondiagonal in  $j$ , coupling states with  $j = 0$  and  $j = 2$ , and as the present investigation is of loss rates from the spin-polarized  $^5\Sigma_g^+$  state, the  $j = 1$  states need not be included in the close-coupled calculation. After detailed manipulation of angular momenta coupling relations, the matrix elements of the spin-dipole interaction can be expressed in the form

$$\begin{aligned} & \langle R, J' M_{J'} j' l' | H_{\text{sd}}(\mathbf{R}) | R, J M_{Jj} l \rangle \\ &= \frac{\mu_0 (g_s \mu_B)^2}{4\pi R^3} C^{\text{sd}}(j, j') D^{\text{sd}}(J, j, j', l, l') \delta_{J, J'} \delta_{M_{J'}, M_{Jj}}, \end{aligned} \quad (18)$$

where



$$C^{\text{sd}}(0,0)=0, \quad C^{\text{sd}}(0,2)=C^{\text{sd}}(2,0)=\sqrt{10},$$

$$C^{\text{sd}}(2,2)=-\sqrt{70},$$

and

$$D^{\text{sd}}(J,j,j',l,l')=[l]^{1/2}C(l2l';000)W(Jj'l2;l'j), \quad (19)$$

$[a]=2a+1$ , and  $W(abcd:ef)$  is a Racah coefficient [43].  
The Hamiltonian for the Zeeman interaction has the form

$$H_{\text{Zee}}=(g_s\mu_B/\hbar)\mathbf{B}\cdot\mathbf{S}=(g_s\mu_B/\hbar)BS_z, \quad (20)$$

where  $\mathbf{B}$  is the magnetic field and it has been assumed that the magnetic field is directed along the space-fixed  $z$  axis. The matrix elements for the Zeeman interaction can be written as

$$\begin{aligned} \langle R,J'M_J,j'l'|H_{\text{Zee}}|R,JM_Jj,l\rangle \\ =g_s\mu_B B C^{\text{Zee}}(j)D^{\text{Zee}}(J,J',M_J,j,l)\delta_{M_J,M_J'}\delta_{j,j'}\delta_{l,l'}, \end{aligned} \quad (21)$$

where

$$C^{\text{Zee}}(0)=0, \quad C^{\text{Zee}}(2)=-\sqrt{10}$$

and

$$\begin{aligned} D^{\text{Zee}}(J,J',M_J,j,l) \\ =(-1)^{l-J'+J-M_J}([j][j'])^{1/2}W(JjJ'j;l1) \\ \times C(JJ'1;M_J,-M_J,0). \end{aligned} \quad (22)$$

### C. Transformed molecular basis

Having considered the matrix elements of the various components of the total Hamiltonian, an appropriate set of molecular basis states may now be constructed. For the specific case of collisions between metastable triplet helium atoms, the explicit expressions for the matrix elements of the radial kinetic energy, rotational, and electronic Hamiltonians, given by Eqs. (13) and (15), show that these matrix elements are diagonal in all quantum numbers associated with the states  $|R,JM_Jj,l\rangle$ . For all components of the total Hamiltonian, including the spin-dipole and Zeeman interactions, for which the matrix elements are given by Eqs. (18) and (21), respectively, the quantum number  $M_J$  is conserved. In the presence of an external field, the total angular momentum  $\mathbf{J}$  is no longer conserved. From Eqs. (21) and (22), it can be seen that for an external magnetic field the Zeeman interaction couples states which are characterized by the same  $j$  and  $l$  quantum numbers but may have different  $J$ , where  $J'=J,J\pm 1$ . Since the spin-dipole interaction couples states which have the same  $J$  but may have different  $j$  and  $l$ , where  $j'=j,j\pm 2$  and  $l'=l,l\pm 2$ , an infinite set of coupled differential equations will result. Truncation of the infinite set of molecular basis states will therefore be required and the contribution of the excluded states must be estimated to determine the error associated with the truncation. It is also necessary to select a molecular basis for which the total

Hamiltonian matrix is asymptotically diagonal. For the total angular momentum states (12), there exist off-diagonal matrix elements of the Zeeman interaction Hamiltonian, and since the Zeeman interaction does not have a dependence on the radial separation, these off-diagonal matrix elements will not vanish asymptotically. A new molecular basis, for which matrix elements of the Zeeman interaction Hamiltonian are diagonal, must therefore be defined.

A new molecular basis is defined for a given set of asymptotically conserved quantum numbers  $M_J,j,l$ :

$$|R,M_Jj,l\alpha\rangle=\sum_{J=l-j}^{l+j}\mathcal{A}_{\alpha J}^{M_Jj,l}|R,JM_Jj,l\rangle, \quad (23)$$

where  $\mathcal{A}_{\alpha J}^{M_Jj,l}$  is obtained by diagonalizing the asymptotic Hamiltonian and  $1\leq\alpha\leq 2j+1$ . The spin-dipole interaction, which couples together states of different  $j$  and  $l$  between the sets of states defined in Eq. (23), is generally small and therefore the infinite set of coupled equations is truncated by neglecting coupling to sets of states with  $l$  values outside a specified range. For this investigation, the exclusion of sets of states other than those with  $l'=l,\pm 2$  provided sufficient accuracy and resulted in a maximum of 18 coupled equations to be solved. The error associated with the truncation process is numerically determined by repeating select calculations with sets of states with  $l'=l,\pm 4$  also included.

As commented upon earlier, it is recognized that in the uncoupled basis, for which the molecular states are  $|j,M_j,l,M_l\rangle$ , the Zeeman interaction is asymptotically diagonal and in fact the numerical transformation of the basis could have been avoided. However, use of the total angular momentum basis for the present study did not impose any significant numerical overheads and the strategy adopted to deal with the infinite set of coupled equations, several aspects of which will be appropriate for a subsequent study of collisions in the presence of an external light field, could be validated against results obtained using the uncoupled basis.

### D. Close-coupled scattering equations

The expansion of the total wave function in terms of the molecular basis given in Eq. (23) and the unknown radial functions  $F_{\alpha j l \gamma, \alpha' j' l \gamma'}^{JM_J}(E,R)$  takes on the form

$$|\Psi_{j'l'\alpha'}^{JM_J}(E,R)\rangle=\sum_j\sum_l\sum_{\alpha=1}^{2j+1}\frac{1}{R}F_{j l \alpha, j' l \alpha'}^{M_J}(E,R)|R,M_Jj,l\alpha\rangle, \quad (24)$$

where  $E$  is the total energy of the system. The close-coupled scattering equations are generated by substituting the total wave function (24) into the time-independent Schrödinger equation and forming the inner product with the individual basis states (23), that is,

$$\langle R,M_Jj''l''\alpha''|(H-E)|\Psi_{j'l'\alpha'}^{M_J}(E,R)\rangle=0. \quad (25)$$

Substitution of Eqs. (23) and (24) into Eq. (25) and using the explicit evaluations (13), (15), (18), and (21) for the Hamiltonian matrix elements, the  $N$  coupled second-order differential scattering equations, for metastable triplet helium atoms in the presence of a magnetic field, are given by

$$\left[ \frac{d^2}{dR^2} - \frac{l''(l''+1)}{R^2} - \frac{2\mu}{\hbar^2} {}^{2S+1}V_{\Sigma}(R) + k_{M_j j'' l'' \alpha''}^2 \right] \times F_{j'' l'' \alpha''; j' l' \alpha'}^{M_j}(E, R) = \frac{2\mu}{\hbar^2} \sum_j \sum_l \sum_{\alpha=1}^{2j+1} V_{j'' l'' \alpha''; j l \alpha}^{\text{sd}}(R) F_{j l \alpha; j' l' \alpha'}^{M_j}(E, R), \quad (26)$$

where

$$k_{M_j j l \alpha}^2 = \frac{2\mu}{\hbar^2} [E - E^\infty - V^{\text{Zee}}(M_j, j, l, \alpha)], \quad (27)$$

$$V^{\text{Zee}}(M_j j l \alpha) = g_s \mu_B B C^{\text{Zee}}(j) \times \sum_{J=l-j}^{l+j} \sum_{J'=l-j}^{l+j} \mathcal{A}_{\alpha J}^{M_j j l} \mathcal{A}_{\alpha J'}^{M_j j l *} \times D^{\text{Zee}}(J, J', M_j, j, l), \quad (28)$$

$$V_{j' l' \alpha'; j l \alpha}^{\text{sd}}(R) = \frac{\mu_0}{4\pi} \frac{(g_s \mu_B)^2}{R^3} C^{\text{sd}}(j, j') \times \sum_{J=l-j}^{l+j} \sum_{J'=l-j'}^{l'+j'} \mathcal{A}_{\alpha J}^{M_j j l} \mathcal{A}_{\alpha' J'}^{M_j j' l' *} \times D^{\text{sd}}(J, j, j', l, l'), \quad (29)$$

and  $D^{\text{sd}}(J, j, j', l, l')$  and  $D^{\text{Zee}}(J, J', M_j, j, l)$  are given by Eqs. (19) and (22), respectively. In Eq. (26), the  $N$  linearly independent solutions are labeled by the singly primed quantities.

For the collisions of metastable triplet helium atoms, Penning ionization occurs at small radial separations from the  $^1\Sigma_g^+$  quasimolecule state. The loss of flux due to Penning ionization is represented in this investigation by a complex optical potential [30], replacing the  $^1V_{\Sigma}(R)$  potential in the electronic Hamiltonian matrix (15) by the complex potential  $^1V_{\Sigma}(R) - i\Gamma(R)/2$ , where  $^1V_{\Sigma}(R)$  is the usual adiabatic molecular potential for the  $^1\Sigma_g^+$  quasimolecule state and  $\Gamma(R)$  is the total autoionization width for the  $\text{He}_2^*(^1\Sigma_g^+)$  entrance channel. As a result of the complex interaction potential, the scattering equations (26) and the solution matrices  $\mathbf{F}(E, R)$  are complex.

The collisions under investigation involve identical atoms and therefore symmetrization requirements must be considered. Following Mies [45], symmetrized channel states were used in these calculations and hence properly symmetrized scattering matrices and cross sections were calculated. This particular collision system involves identical nuclei of zero spin and the symmetrization of the channel states has the consequences that only gerade states of the molecule and even partial wave values contribute to the scattering process. No significant alteration is therefore required of the theory developed above.

### E. Scattering matrices, cross sections, and rate constants

The scattering matrix is determined from the asymptotic form of the matrix of radial functions  $\mathbf{F}(E, R)$ , which is given by

$$\mathbf{F}(E, R) \underset{R \rightarrow \infty}{\sim} \mathbf{J} + \mathbf{N} \mathbf{K}, \quad (30)$$

where  $\mathbf{J}$  and  $\mathbf{N}$  are real diagonal matrices with elements

$$J_{ij} = k_i^{1/2} R j_{l_i}(k_i R) \delta_{ij}, \\ N_{ij} = -k_i^{1/2} R n_{l_i}(k_i R) \delta_{ij}, \quad (31)$$

and  $j_{l_i}(k_i R)$  and  $n_{l_i}(k_i R)$  are regular and irregular spherical Bessel functions. The reactance matrix  $\mathbf{K}$  will be complex as a result of  $\mathbf{F}(E, R)$  being complex.

The required scattering matrix  $\mathbf{S}$  is obtained from the reactance matrix  $\mathbf{K}$  by

$$\mathbf{S} = (\mathbf{I} + i\mathbf{K})(\mathbf{I} - i\mathbf{K})^{-1}, \quad (32)$$

where  $\mathbf{I}$  is the  $N \times N$  identity matrix.

The scattering cross section for the transition from state  $\gamma_i$  to  $\gamma_f$ , where  $\gamma = \{j, M_j\}$ , is given by

$$\sigma(E; \gamma_i \rightarrow \gamma_f) = \frac{\pi}{k_i^2} \sum_{l_i, M_{l_i}, l_f, M_{l_f}} |T(E; \beta_i \rightarrow \beta_f)|^2, \quad (33)$$

where  $\beta = \{j, M_j, l, M_{l_i}\}$ ,  $T(E; \beta_i \rightarrow \beta_f)$  are the transition matrix elements and the transition matrix  $\mathbf{T}$  is related to the scattering matrix  $\mathbf{S}$  via  $\mathbf{T} = \mathbf{I} - \mathbf{S}$ . For the present investigation,  $M_{j_i} = M_{j_f}$  and therefore the summation over  $M_{l_f}$  is restricted by the condition  $M_{l_i} + M_{j_i} = M_{l_f} + M_{j_f}$ .

The calculation of the collision cross section for the relaxation-induced Penning ionization process requires the probability of the transition from the  $j=2$ ,  $M_j=2$  initial state to all possible ionization channels. In the present calculations, the loss of flux due to Penning ionization has been represented by a complex potential which is assumed equivalent to coupling in the ionization channels. Thus the scattering matrix element for Penning ionization from the initial state can be obtained from the calculated, nonunitary  $N \times N$  scattering matrix:

$$|S_{\Gamma_i \rightarrow \Gamma_{pl}}|^2 = 1 - \sum_{\Gamma'=1, N} |S_{\Gamma_i, \Gamma'}|^2, \quad (34)$$

where  $\Gamma_i$  is the initial scattering channel.

The rate coefficient for the transition  $\gamma_i \rightarrow \gamma_f$  is given by

$$K(T, \gamma_i \rightarrow \gamma_f) = \langle \sigma(E, \gamma_i \rightarrow \gamma_f) v_i \rangle, \quad (35)$$

where  $v_i = \hbar k_i / \mu = (2E/\mu)^{1/2}$  and the angular brackets in Eq. (35) denote an average over the distribution of the relative velocities of the colliding atoms. For very low temperatures where quantum threshold behavior becomes applicable, this averaging over relative velocities is no longer required and the rate coefficient expressions can be simplified to give

$$K(T, \gamma_i \rightarrow \gamma_f) \sim \begin{cases} \sigma(E, \gamma_i \rightarrow \gamma_f) v_i, & \gamma_i \neq \gamma_f \\ \left(\frac{8E}{\mu\pi}\right)^{1/2} \sigma(E, \gamma_i \rightarrow \gamma_f), & \gamma_i = \gamma_f \end{cases} \quad (36)$$

In Sec. IV, rate constants for elastic scattering and for the loss of atoms as a result of inelastic processes will be reported. For identical atoms, this involves a factor of 2 times the rate constants given in Eqs. (35) and (36) since two atoms are lost per collision event.

### III. NUMERICAL CALCULATIONS

A modified version of the FARM package [42] was employed to solve the coupled second-order linear differential equations (26) and to obtain the required transition matrices. The FARM package incorporates a combination of  $\mathcal{R}$ -matrix propagation techniques, where  $\mathcal{R} = \mathbf{F}(d\mathbf{F}/dR)^{-1}$ , to integrate the coupled Schrödinger equations, and matching of the solution to an asymptotic wave function, which is determined by an accelerated Gailitis expansion. The accelerated Gailitis expansion is used to minimize the radial distance at which the matching procedure can be undertaken and hence reduce the range over which the scattering equations must be integrated.

Significant modification of the original FARM package was required to incorporate a complex interaction potential. The solutions of the coupled equations are now complex and therefore propagation of a complex  $\mathcal{R}$  matrix is required. The FARM package was also modified to enable the transformation of the molecular basis during the calculation and to allow direct integration of the coupled equations out to the asymptotic region where the solutions could be matched to the free-field solutions, as an alternative to the use of the accelerated Gailitis expansion routines. Due to the presence of terms involving inverse powers of  $k$  and the energy separation between scattering channels in the recursion relations for the Gailitis expansion coefficients, a breakdown in the performance of the Gailitis routines was found for calculations at very low scattering energies and for small energy separations between scattering channels.

The performance of the FARM package was favorable for the calculations undertaken. A large range of temperatures was considered in this investigation and for the higher temperatures, where the distribution of the relative velocities of the colliding atoms was considered important, and solutions to the close-coupled equations were required for a large number of energies. The  $\mathcal{R}$ -matrix propagation routines have the advantage that the most computationally demanding parts of these methods, namely the diagonalization of the total Hamiltonian or interaction Hamiltonian matrices, are energy independent. As well as being computationally efficient,  $\mathcal{R}$ -matrix propagation techniques provide high numerical stability for the integration of coupled equations describing atomic collision processes. With the exception of those cases where a breakdown in the performance of the Gailitis routines was expected because of the relative size of the terms in the recursion relations, the Gailitis routines were found to work well, enabling scattering boundary conditions to be imposed at smaller radial separations than would normally be required for the low temperatures under investigation.

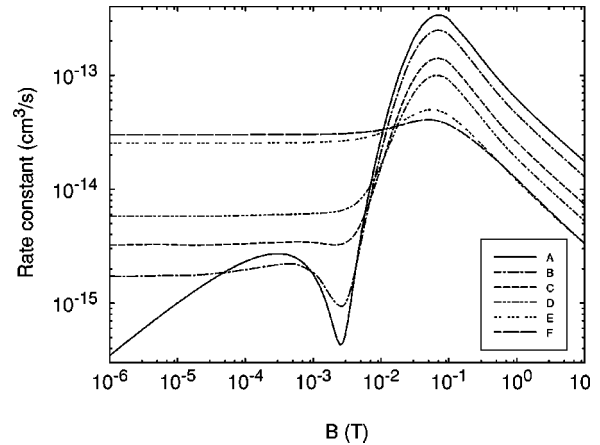


FIG. 1. Spin-relaxation rate constants as a function of  $B$  for a range of temperatures: (A)  $T=1$  nK, (B)  $T=1$  mK, (C)  $T=5$  mK, (D)  $T=10$  mK, (E)  $T=50$  mK, and (F)  $T=100$  mK.

At the higher collision energies and for the lower range of values of magnetic field considered in this investigation, many partial waves (as many as 20) were found to contribute to the collision cross section. Accelerated convergence techniques were applied to slowly converging summations over initial partial wave values  $l_i$  appearing in Eq. (33) to avoid computation of transition matrix elements for higher partial wave values. The two methods chosen, the Levin  $u$ -transform and the  $\theta$  algorithm [46], are particularly suited to monotone series and in a detailed comparison made by Smith and Ford [46] were rated as two of the three overall best accelerated convergence methods.

The chosen truncated molecular basis and the routines in the FARM package enabled at least four significant figures of accuracy to be maintained in the propagation of the  $\mathcal{R}$  matrix. However, near cancellation of terms in the matching of the solutions to the asymptotic form at lower temperatures reduced the accuracy obtained for the scattering matrices to approximately three significant figures. This loss of accuracy could not be attributed to the use of the Gailitis routines and was shown to also occur when the  $\mathcal{R}$  matrix was propagated to larger separations and matched to the free-field solutions. The results reported in the following section were therefore accurate to better than 1% for all temperatures and magnetic fields considered.

### IV. RESULTS AND DISCUSSION

In this section the results of the close-coupled calculations will be presented and compared with the only other existing results for magnetostatically trapped metastable helium atoms [12,13]. The sensitivity of the calculated collision rate constants to the input molecular potentials and autoionization width will be assessed. This is essential because extraordinary accuracy is required of molecular potentials for ultracold collision calculations, exceeding that of available molecular potentials, and no full theoretical treatments of the autoionization processes exist.

The calculation by Fedichev *et al.* [12,13] is based on a first-order perturbative treatment of the spin-dipole term and is equivalent to a distorted Born wave treatment. Although one would like to make a detailed comparison between this

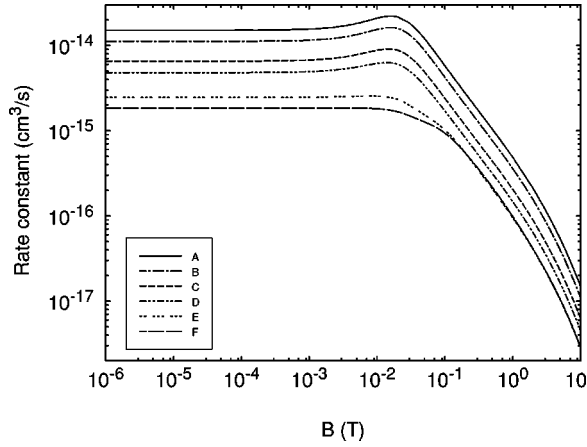


FIG. 2. Relaxation-induced Penning ionization rate constants as a function of  $B$  for a range of temperatures: (A)  $T=1$  nK, (B)  $T=1$  mK, (C)  $T=5$  mK, (D)  $T=10$  mK, (E)  $T=50$  mK, and (F)  $T=100$  mK.

approach and the quantum close-coupled method, the sensitivity of the results to both the molecular potentials and the representation of the flux loss due to Penning ionization, and the absence of any experimental data, would not enable many valuable conclusions to be drawn. However, it is believed that observation of the differences between the results obtained using these two different approaches is worthwhile, particularly in the cases where loss rates differ significantly from those predicted previously.

The rate constants for the spin relaxation (SR) and relaxation-induced Penning ionization (RIPI) processes as a function of magnetic field and for a range of temperatures are shown, respectively, in Fig. 1 and Fig. 2 and exhibit the same general features as the corresponding figures given by Fedichev *et al.* [12]. However, there are some differences in rate-constant values for the inelastic processes. The SR rate constants for  $B \geq 10$  mT ( $1 \text{ G} = 10^{-4} \text{ T}$ ) and  $T \leq 10$  mK are at least a factor of 1.5 smaller than those reported by Fedichev *et al.*, and the minimum shown in Fig. 1 at  $B \approx 2.5$  mT was found by Fedichev *et al.* to occur at a lower magnetic field value than that reported here. Although the origin of these differences is not specifically known, it will be shown later that a small variation of the  ${}^5\Sigma_g^+$  molecular potential can produce these types of differences. The RIPI rate constants reported by Fedichev *et al.*, for all temperatures and magnetic fields, are a factor of 1.5–2 larger than shown in Fig. 2. This is expected because the autoionization width used as the imaginary part of the complex potential represents less loss of flux due to Penning ionization than the perfectly absorbing boundary used by Fedichev *et al.* The elastic rate constants, which were found to not vary with magnetic field, are tabulated in Table I for a range of temperatures and are in close agreement with those calculated by Fedichev *et al.*

To investigate the sensitivity of the results to the autoion-

TABLE I. Elastic scattering rate constants ( $\text{cm}^3 \text{ s}^{-1}$ ) for a range of temperatures.

$T=1$ nK	$T=1$ $\mu\text{K}$	$T=1$ mK	$T=10$ mK	$T=100$ mK
$5.6 \times 10^{-12}$	$1.8 \times 10^{-10}$	$3.5 \times 10^{-9}$	$2.4 \times 10^{-9}$	$1.0 \times 10^{-8}$

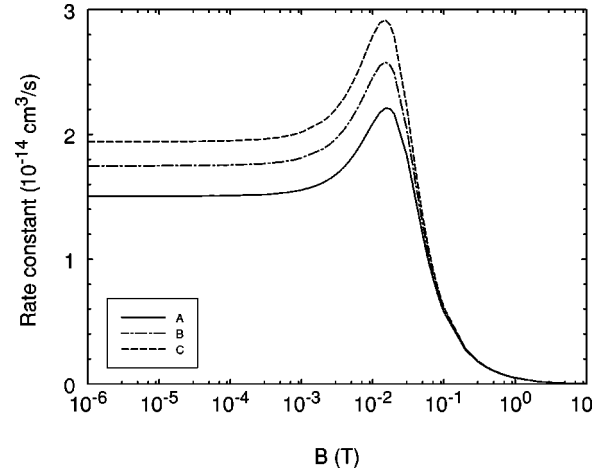


FIG. 3. Relaxation-induced Penning ionization rate constants as a function of  $B$  at  $T=1$  nK for various autoionization widths: (A)  $\Gamma(R)$ , (B)  $\Gamma_{\text{GMS}}(R)$ , and (C)  $\Gamma_{\text{UP}}(R)$ .

ization width, some of the calculations for a range of magnetic fields and temperatures were repeated using the autoionization width  $\Gamma_{\text{GMS}}(R) = 0.3 \exp(-R/1.086)$  suggested by Garrison *et al.* [47], which exhibits a steeper exponential behavior and does not dampen at small internuclear separations like that of Müller *et al.* [30]. Spin-relaxation transitions which remain in the  ${}^5\Sigma_g^+$  quasimolecular state are generally dominant over those which relax to the  ${}^1\Sigma_g^+$  state and therefore the sum of the rate constants for the SR processes did not alter significantly with variation of the autoionization width, which is coupled directly to the  ${}^1\Sigma_g^+$  state. For  $T \leq 10$  mK and  $B \leq 15$  mT, the rate constants for RIPI were found to be  $\approx 16\%$  greater using  $\Gamma_{\text{GMS}}(R)$ . Results for  $T=1$  nK are shown in Fig. 3, together with results obtained using an autoionization width  $\Gamma_{\text{UP}}(R)$  constructed to simulate unit probability of Penning ionization within some internuclear separation  $R = \bar{R}$ :

$$\Gamma_{\text{UP}}(R) = \begin{cases} \Gamma_{\text{GMS}}(R) + (R - \bar{R})^2 e^{-cR} & \text{for } R \leq \bar{R} \\ \Gamma_{\text{GMS}}(R) & \text{for } R > \bar{R}. \end{cases} \quad (37)$$

The results are insensitive to variation of  $\bar{R}$  and  $c$  within the ranges  $6 \leq \bar{R} \leq 7 a_0$  and  $0.5 \leq c \leq 1$ , supporting the assumption that the form given in Eq. (37) does actually simulate total loss of flux within a particular internuclear separation. The RIPI rate constants calculated using  $\Gamma_{\text{UP}}(R)$  are as much as 30% greater than those obtained using  $\Gamma(R)$  but still approximately 20% smaller than those reported by Fedichev *et al.*

The analytical form of the  ${}^5\Sigma_g^+$  potential given by Starck and Meyer [41] was used for the quantum close-coupled calculations. More accurate dispersion coefficients [48] than those used in this analytical expression [49] are now available and were used to assess the influence of the long-range potential on the results. The short-range singlet  ${}^1V_\Sigma(R)$  and quintet  ${}^5V_\Sigma(R)$  potentials for  $R \leq 20 a_0$  were left unaltered and smoothly connected onto the long-range  $-C_6 R^{-6} - C_8 R^{-8} - C_{10} R^{-10}$  form of Yan and Babb [48], and it was found that the rate constants altered by less than 0.5%. Since the short-range  ${}^5\Sigma_g^+$  potential is estimated to be accurate to



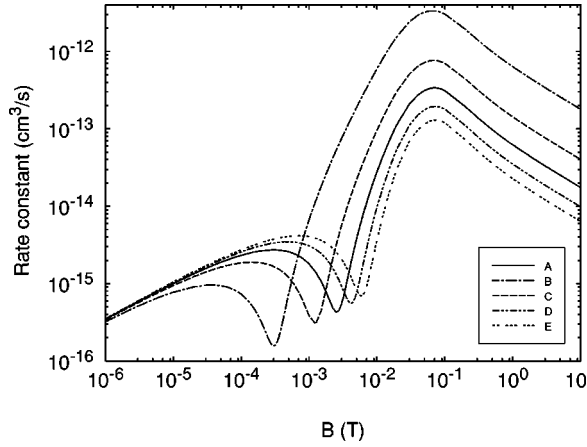


FIG. 4. Spin-relaxation rate constants as a function of  $B$  at  $T = 1$  nK for (A) no variation, (B) +1%, (C) -1%, (D) +0.5%, and (E) -0.5% variation of the short-range  ${}^5V_{\Sigma}(R)$  potential.

within 1% [41], the short-range singlet and quintet potentials were varied for  $R \leq 14 a_0$  within this 1% accuracy and smoothly connected onto the unaltered long-range form. It has been shown [50] that within the  $\pm 1\%$  variation of the potentials, the number of bound states does not change. The results for  $T \leq 1$  mK were most affected. The SR and RIPI rate constants for  $T = 1$  nK, shown in Fig. 4 and Fig. 5, respectively, vary significantly with the different modifications to the molecular potentials. The SR rate constants displayed little sensitivity to the short-range form of the  ${}^1\Sigma_g^+$  potential and from Fig. 5 it can be seen that, although the rate constants for RIPI showed some sensitivity, the results are much more dependent on the short-range  ${}^5\Sigma_g^+$  potential.

Study of the sensitivity of the potentials for  $T > 1$   $\mu$ K was limited to a select number of magnetic fields and temperatures across the total range under investigation because of the computational effort required in redoing a full set of calculations. From these, the following estimates have been made for the possible range of variation of the rate constants within the accuracy of the potentials. For the range of magnetic fields  $B \geq 10$  mT, for which SR is the dominant inelas-

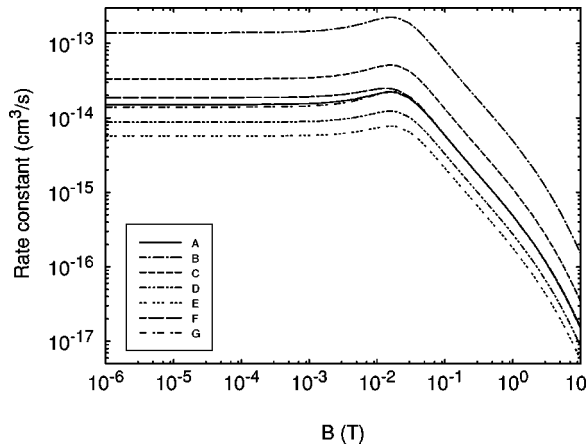


FIG. 5. Relaxation-induced Penning ionization rate constants as a function of  $B$  at  $T = 1$  nK for (A) no variation, (B) +1%, (C) -1%, (D) +0.5%, (E) -0.5% variation of the short-range  ${}^5V_{\Sigma}(R)$  potential, and (F) +1%, and (G) -1% variation of the short range  ${}^1V_{\Sigma}(R)$  potential.

TABLE II. Elastic scattering rate constants ( $\text{cm}^3 \text{s}^{-1}$ ) at  $T = 1$  nK for several variations of the short-range  ${}^5V_{\Sigma}(R)$  potential.

No variation	1%	0.5%	-0.5%	-1%
$5.6 \times 10^{-12}$	$4.4 \times 10^{-11}$	$1.2 \times 10^{-11}$	$3.5 \times 10^{-12}$	$2.4 \times 10^{-12}$

tic process at all temperatures considered, variation of the short-range quintet potential within 1% for  $T \leq 1$  mK yielded either increases in the SR rate constants by a factor greater than 2.5, and as large as 10 for  $T \leq 1$   $\mu$ K, or a decrease by approximately a factor of 2. At higher temperatures ( $T \geq 1$  mK), the variation of the rate constants for SR is likely to be, at most, a factor of 1.6. Relaxation-induced Penning ionization is the dominant inelastic process for  $B \leq 10$  mT and  $T \leq 7.5$  mK. Within the accuracy of the potentials, the RIPI rate constants could be a factor of 9 larger or a factor of at least 2.6 smaller for  $T \leq 1$   $\mu$ K. For  $1$   $\mu$ K  $\leq T \leq 7.5$  mK, an increase in the RIPI rate constant values by a factor of approximately 2.5 and a decrease by a factor of 1.25 could also be possible. For  $B \leq 10$  mT and  $T \geq 7.5$  mK, SR once again governs the total loss rates with possible variation on the values shown in Fig. 1 by a factor of 1.5–2.

The response of the elastic rate constants at  $T = 1$  nK to modifications of the short-range  ${}^5\Sigma_g^+$  molecular potential is shown in Table II. An increase by at least a factor of 7.5 or a decrease by at least a factor of 2 in the elastic rate constants given in Table I could be possible for  $T \leq 1$   $\mu$ K and, for  $1$   $\mu$ K  $\leq T \leq 1$  mK, there could be approximately a factor of 2 difference. For higher temperatures,  $T \geq 1$  mK, the reported elastic rate constants are predicted to alter by less than 10% within the accuracy of the molecular potentials.

The ratios of the elastic to inelastic rates at  $T = 1$  nK are displayed in Fig. 6 and, although small variations of the molecular potentials can produce large changes in the rate constants, it can be seen from Fig. 6 that the ratio of the elastic to inelastic rates is much less sensitive. The sensitivity of the rate constants to variation of the  ${}^5\Sigma_g^+$  molecular potential by a multiplicative factor of 1.01 was considered by Fedichev *et al.* [12,13], who found similar effects.

Fedichev *et al.* [12,13,51] discuss the importance of three-body recombination to a weakly bound  $s$  level for ul-

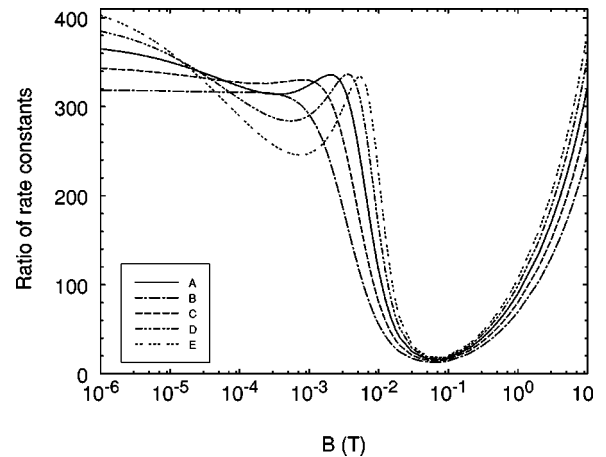


FIG. 6. Ratio of elastic to inelastic rates as a function of  $B$  at  $T = 1$  nK for (A) no variation, (B) +1%, (C) -1%, (D) +0.5%, and (E) -0.5% variation of the short range  ${}^5V_{\Sigma}(R)$  potential.

tralow temperatures  $T \ll \epsilon_0$ , where  $\epsilon_0$  is the binding energy, and conclude that two-body inelastic processes dominate for gas densities  $n \lesssim 10^{13} \text{ cm}^{-3}$ . The three-body recombination rate varies strongly with the scattering length  $a$  as  $a^4$  [51], and since small variations of the  ${}^5\Sigma_g^+$  potential within the claimed 1% accuracy can significantly vary both the scattering length [50] and the loss rates for two-body inelastic processes, it is possible that the restrictions on gas density, which eliminate three-body recombination as the dominating process, could be more stringent than predicted by Fedichev *et al.* [12,13].

## V. SUMMARY

A close-coupled calculation has been undertaken to produce rate constants for elastic scattering and the spin-relaxation and relaxation-induced Penning ionization processes for a range of temperatures and magnetic fields. This investigation has been motivated, in part, by the desire to extend this calculational strategy to a study of collisions of metastable helium atoms in the presence of an optical field. The calculated rate constants exhibit the same general behavior as results produced by Fedichev *et al.* [12,13]. However,

some results for the inelastic processes were found to be at least a factor of 1.5 smaller than those reported previously. The results were found to be sensitive to the short-range molecular potentials and the autoionization width, but as concluded by Fedichev *et al.* [12,13], the ratio of the elastic to inelastic rates was found to be relatively insensitive to variation of the  ${}^5\Sigma_g^+$  potential, upon which the results were most dependent. To obtain more reliable theoretical results, molecular potentials are required to a greater accuracy and more detailed theoretical studies of the autoionization processes are necessary.

## APPENDIX: MATRIX ELEMENTS OF THE HAMILTONIAN COMPONENTS

Explicit evaluations of matrix elements of the various terms in the total Hamiltonian are obtained using the expressions for the channel states given in either Eq. (9) or Eq. (12).

Using the expansion of the molecular states given by Eqs. (11) and (12), and the relation (14), the matrix elements of the electronic Hamiltonian are

$$\begin{aligned}
 \langle R, J' M_{J'} j' l' | H_{\text{el}} | R, J M_J j l \rangle &= \frac{([l][l'])^{1/2}}{4\pi} \sum_{\Omega_j \Omega_{j'}} C(j l J; \Omega_j 0 \Omega_j) C(j' l' J'; \Omega_{j'} 0 \Omega_{j'}) \\
 &\times \int d\Omega_R D_{M_J, \Omega_j}^{J*}(\phi, \theta, 0) D_{M_{J'}, \Omega_{j'}}^{J'}(\phi, \theta, 0) \langle R, j' \Omega_{j'} | (H_1 + H_2 + H_{12}) | R, j \Omega_j \rangle \\
 &= \frac{([l][l'])^{1/2}}{[J]} \sum_{\Omega_j} C(j l J; \Omega_j 0 \Omega_j) C(j' l' J'; \Omega_{j'} 0 \Omega_{j'}) \sum_{\Omega_L \Omega_S} C(L S j; \Omega_L \Omega_S \Omega_j) C(L S j'; \Omega_L \Omega_S \Omega_{j'}) \\
 &\times [E^\infty + {}^{2S+1}V_\Lambda(R)] \delta_{J, J'} \delta_{M_J, M_{J'}}, \tag{A1}
 \end{aligned}$$

where  $[a] = 2a + 1$ .

The matrix elements of the spin-dipole interaction, given by Eq. (17), between the quasimolecular spin states can be written, after detailed manipulation of angular momenta coupling relations, as

$$\begin{aligned}
 \langle S' M_{S'} | H_{\text{sd}} | S M_S \rangle &= \frac{\mu_0 (g_s \mu_B)^2}{4\pi R^3} 2\sqrt{6\pi} \{S^{(1)}(S^{(1)}+1)S^{(2)}(S^{(2)}+1)[S^{(1)}][S^{(2)}][S]\}^{1/2} F(S^{(1)}, S^{(2)}; S, S') \\
 &\times (-1)^{M_{S'} - M_S} C(S 2 S'; M_S, M_{S'} - M_S, M_{S'}) Y_{2, M_S - M_{S'}}(\hat{\mathbf{R}}), \tag{A2}
 \end{aligned}$$

where

$$F(S^{(1)}, S^{(2)}; S, S') = \sum_f [f] W(S^{(1)} S^{(1)} 2 1; 1 f) W(f S^{(1)} S^{(2)} S^{(2)}; 1 S') W(S S^{(1)} S' f; S^{(2)} 2). \tag{A3}$$

Using the expansions of the channel states given in Eqs. (4) and (9), the matrix elements for the spin-dipole interaction are

$$\begin{aligned}
\langle R, J' M_{J'} j' l' | H_{\text{sd}} | R, J M_{Jj} l \rangle &= \frac{\mu_0 (g_s \mu_B)^2}{4\pi R^3} \sqrt{30} \{S^{(1)}(S^{(1)}+1)S^{(2)}(S^{(2)}+1)[S^{(1)}][S^{(2)}][S]\}^{1/2} F(S^{(1)}, S^{(2)}; S, S') \\
&\times \left( \frac{[l]}{[l']} \right)^{1/2} C(l2l'; 000) \sum_{M_j M_{j'}} C(jlJ; M_j, M_J - M_j, M_J) C(j'l'J'; M_{j'}, M_{J'} - M_{j'}, M_{J'}) \\
&\times \sum_{M_S M_{S'}} (-1)^{M_{S'} - M_S} C(LSj; M_j - M_S, M_S M_j) C(LS'j'; M_{j'} - M_{S'}, M_{S'} M_{j'}) \\
&\times C(S2S'; M_S, M_{S'} - M_S, M_{S'}) C(l2l'; M_J - M_j, M_S - M_{S'}, M_{J'} - M_{j'}), \quad (\text{A4})
\end{aligned}$$

where  $F(S^{(1)}, S^{(2)}; S, S')$  is given by Eq. (A3).

The Hamiltonian for the Zeeman interaction is given by Eq. (20) and using the expression (9) for the channel states and the expansion (4), together with the orthonormality relation of the spherical harmonics [52], the matrix elements for the Zeeman interaction become

$$\begin{aligned}
\langle R, J' M_{J'} j' l' | H_{\text{Zee}} | R, J M_{Jj} l \rangle &= g_s \mu_B B (-1)^{j+j'+l-J'} [J]^{1/2} \sum_g [g]^{1/2} W(JjJ'j'; lg) C(JgJ'; M_J 0 M_J) \\
&\times \sum_{M_j} (-1)^{M_j} C(jj'g; -M_j, M_j, 0) \\
&\times \sum_{M_S} C(LSj; M_j - M_S, M_S M_j) C(LS'j'; M_j - M_S, M_S M_j) M_S \delta_{M_J, M_{J'}} \delta_{l, l'}. \quad (\text{A5})
\end{aligned}$$

- 
- [1] M. H. Anderson *et al.*, *Science* **269**, 198 (1995).  
[2] H. Metcalf and P. van der Straten, *Phys. Rep.* **244**, 203 (1994).  
[3] P. S. Julienne and F. H. Mies, *J. Opt. Soc. Am. B* **6**, 2257 (1989).  
[4] J. Weiner, in *Advances in Atomic, Molecular and Optical Physics*, edited by B. Bederson and H. Walther (Academic Press, San Diego, CA, 1995), Vol. 35, pp. 45–78.  
[5] A. Aspect *et al.*, *Phys. Rev. Lett.* **61**, 826 (1988).  
[6] H. Metcalf, *J. Opt. Soc. Am. B* **6**, 2206 (1989).  
[7] N. Morita and M. Kumakura, *Jpn. J. Appl. Phys., Part 2* **30**, L1678 (1991).  
[8] C. Westbrook *et al.*, in *TENICOLS '91*, papers presented at the Tenth International Conference on Laser Spectroscopy, France, June, 1991, edited by E. G. M. Ducloy and G. Camy (World Scientific, Singapore, 1991), pp. 48 and 49.  
[9] M. Kumakura and N. Morita, *Jpn. J. Appl. Phys., Part 2* **31**, L276 (1992).  
[10] J. Lawall *et al.*, *Phys. Rev. Lett.* **75**, 4194 (1995).  
[11] R. Schumann *et al.*, *Phys. Rev. A* **59**, 2120 (1999).  
[12] P. O. Fedichev, M. W. Reynolds, U. M. Rahmanov, and G. V. Shlyapnikov, *Phys. Rev. A* **53**, 1447 (1996).  
[13] G. V. Shlyapnikov, J. T. M. Walraven, U. M. Rahmanov, and M. W. Reynolds, *Phys. Rev. Lett.* **73**, 3247 (1994).  
[14] A. Aspect *et al.*, *Chem. Phys.* **145**, 307 (1990).  
[15] M. D. Hoogerland *et al.*, *Aust. J. Phys.* **49**, 567 (1996).  
[16] F. Bardou *et al.*, *Europhys. Lett.* **20**, 681 (1992).  
[17] H. C. Mastwijk, J. W. Thomsen, P. van der Straten, and A. Neihaus, *Phys. Rev. Lett.* **80**, 5516 (1998).  
[18] M. Kumakura and N. Morita, *Phys. Rev. Lett.* **82**, 2848 (1999).  
[19] K. G. H. Baldwin (private communication).  
[20] F. Shimuzu, K. Shimuzu, and H. Takuma, *Phys. Rev. A* **39**, 2758 (1989).  
[21] H. Katori and F. Shimizu, *Phys. Rev. Lett.* **70**, 3545 (1993).  
[22] M. Walhout *et al.*, *Phys. Rev. Lett.* **74**, 506 (1995).  
[23] H. Katori and F. Shimizu, *Phys. Rev. Lett.* **73**, 2555 (1994).  
[24] H. Kunugita, T. Ido, and F. Shimizu, *Phys. Rev. Lett.* **73**, 621 (1997).  
[25] J. Lawall, C. Orzel, and S. Rolston, *Phys. Rev. Lett.* **80**, 480 (1998).  
[26] C. J. Williams and P. S. Julienne, Theory of Penning Ionization of Metastable He, presented at the Symposium on Cold Atom Collisions, Cambridge, MA, 1992 (unpublished).  
[27] K. A. Suominen *et al.*, *Phys. Rev. A* **53**, 1678 (1996).  
[28] P. S. Julienne, A. M. Smith, and K. Burnett, in *Advances in Atomic, Molecular and Optical Physics*, edited by D. R. Bates and B. Bederson (Academic Press, San Diego, CA, 1993), Vol. 30, pp. 141–199.  
[29] M. W. Müller *et al.*, *Phys. Rev. Lett.* **59**, 2279 (1987).  
[30] M. W. Müller *et al.*, *Z. Phys. D* **21**, 89 (1991).  
[31] R. J. Bieniek, *Phys. Rev. A* **18**, 392 (1978).  
[32] R. W. Heather and P. S. Julienne, *Phys. Rev. A* **47**, 1887 (1993).  
[33] K. A. Suominen, *J. Phys. B* **29**, 5981 (1996).  
[34] K. A. Suominen *et al.*, *Phys. Rev. A* **57**, 3724 (1998).  
[35] J. Weiner, V. S. Bagnato, S. Zilio, and P. Julienne, *Rev. Mod. Phys.* **71**, 1 (1999).  
[36] K. A. Suominen, M. J. Holland, K. Burnett, and P. S. Julienne, *Phys. Rev. A* **51**, 1446 (1995).  
[37] H. M. J. M. Boesten, B. J. Verhaar, and E. Tiesinga, *Phys. Rev. A* **48**, 1428 (1993).  
[38] H. M. J. M. Boesten and B. J. Verhaar, *Phys. Rev. A* **49**, 4240 (1994).  
[39] P. S. Julienne, K. A. Suominen, and Y. Band, *Phys. Rev. A* **49**, 3890 (1994).

- [40] Y. B. Band *et al.*, Phys. Rev. A **50**, R2826 (1994).
- [41] J. Stärck and W. Meyer, Chem. Phys. Lett. **225**, 229 (1994).
- [42] V. M. Burke and C. J. Noble, Comput. Phys. Commun. **85**, 471 (1995).
- [43] M. E. Rose, *Elementary Theory of Angular Momentum*, 1st ed. (John Wiley and Sons, New York, 1957).
- [44] B. H. Bransden and C. J. Joachain, *Physics of Atoms and Molecules*, 1st ed. (Longman Group, London, 1983).
- [45] F. H. Mies (unpublished).
- [46] D. A. Smith and W. F. Ford, SIAM (Soc. Ind. Appl. Math.) J. Numer. Anal. **16**, 223 (1979).
- [47] B. J. Garrison, W. H. Miller, and H. F. Schaefer, J. Comput. Phys. **59**, 3193 (1973).
- [48] Z. Yan and J. F. Babb, Phys. Rev. A **58**, 1247 (1998).
- [49] D. Spelsberg and W. Meyer, J. Comput. Phys. **99**, 8351 (1993).
- [50] J. Babb, P. J. Leo, V. Venturi, and I. Whittingham (unpublished).
- [51] P. O. Fedichev, Y. Kagan, G. V. Shlyapnikov, and J. T. M. Walraven, Phys. Rev. Lett. **77**, 2913 (1996).
- [52] D. M. Brink and G. R. Satchler, *Angular Momentum*, 2nd ed. (Clarendon Press, Oxford, 1968).